

WEC³: Wave Energy Converter Code Comparison Project

Adrien Combourieu¹, Michael Lawson², Aurélien Babarit³, Kelley Ruehl⁴, André Roy⁵,
Ronan Costello⁶, Pauline Laporte Weywada⁷, Helen Bailey⁸

¹*INNOSEA*

1 rue de la Noë, CS12102, 44321 Nantes Cedex 03, France
adrien.combourieu@innosea.fr

²*National Renewable Energy Laboratory (NREL)*

15013 Denver West Parkway, Golden, CO 80401
michael.lawson@nrel.gov

³*Ecole Centrale de Nantes, LHEEA (ECN/CNRS)*

1 rue de la Noë, 44321 Nantes Cedex 03, France
aurelien.babarit@ec-nantes.fr

⁴*Sandia National Laboratories (SNL)*

Albuquerque, NM 87185
kelley.ruehl@sandia.gov

⁵*Dynamic System Analysis Ltd.*

101-19 Dallas Road, Victoria, BC, Canada, V8V 5A6
andre.roy@dsa-ltd.ca

⁶*Wave-Venture*

DoES Liverpool, Gostins Building, Hanover St. L1 4LN,
UKronan@wave-venture.com

⁷*DNV GL*

St. Vincent's Works, Silverthorne Lane, Bristol. BS2 0QD
pauline.veywada@dnvgl.com

⁸*University of Victoria*

POBox 1700 STN CSC, Victoria, BC, V8W 3P6, Canada
hlbailey@uvic.ca

I. ABSTRACT

This paper describes the recently launched Wave Energy Converter Code Comparison (WEC3) project and present preliminary results from this effort. The objectives of WEC3 are to verify and validate numerical modelling tools that have been developed specifically to simulate wave energy conversion devices and to inform the upcoming IEA OES Annex VI Ocean Energy Modelling Verification and Validation project. WEC3 is divided into two phases. Phase I consists of a code-to-code verification and Phase II entails code-to-experiment validation.

WEC3 focuses on mid-fidelity codes that simulate WECs using time-domain multibody dynamics methods to model device motions and hydrodynamic coefficients to model hydrodynamic forces. Consequently, high-fidelity numerical modelling tools, such as Navier-Stokes computational fluid dynamics simulation, and simple frequency domain modelling tools were not included in the WEC3 project.

Keywords— Wave energy converter, multibody dynamics, numerical simulation, code comparison, code validation, code verification, power production assessment

II. INTRODUCTION

The tremendous amount of energy contained in ocean waves [1] is leading private and public organizations across the globe to invest in the development of wave energy converter (WEC) technologies. Experience from the wind energy industry shows that verified and validated numerical modeling tools

are needed to design, analyze, and optimize WEC devices in an accurate, cost efficient, and timely manner [2].

Over the last decade, several WEC specific modeling software tools have been developed to meet the needs of the WEC industry and research community. These software tools model the complex interactions between multi-body dynamics, hydrodynamics, hydrostatics, power-take off systems, and control systems in a coupled simulation environment. Given the complexity of physical phenomena modeled by WEC simulation codes and the fact that many design decisions are based heavily on predictions from these codes, it is exceedingly important to verify and validate code accuracy. The Wave Energy Converter Code Comparison (WEC3) project was recently initiated to meet this need. In addition, the WEC3 project has the objective of informing the upcoming IEA Annex VI Ocean Energy Modelling Verification and Validation project. Furthermore, WEC3 will help identify areas where existing codes need to be improved and what additional research is needed to advance the state of WEC modeling. In order to make the results from this project as beneficial as possible to the research community, all results and data sets will be made publicly available at the conclusion of the project.

WEC3 is focused on the verification and validation of mid-fidelity modeling codes that simulate WECs using time-domain multibody dynamic methods that are coupled with hydrodynamics models that rely on frequency domain hydrodynamic coefficients and viscous drag coefficients to determine hydrodynamic forcing. The WEC3 team made the decision not to consider high-fidelity numerical methods (e.g. Navier-Stokes Computational Fluid Dynamics) because the

research community currently relies heavily on mid-fidelity codes and, therefore, validating and verifying these codes will have immediate relevance and benefit to the community.

WEC3 is a one-year project that was initiated in October 2014 and is divided into two phases. Phase I is a code-to-code comparison effort between the four participating codes described in the next section. During Phase I, participants are modeling a floating three-body flap device described in Section IV. Phase II will consist of a code-to-experiment comparison and the WEC3 team is currently working to identify the best publically available experimental data sets for use in Phase II.

In this paper, the different software tools being used in the WEC3 project are presented. Code features and capabilities are described, and similarities and differences are highlighted.

Next, the code-to-code verification case is discussed. Specifically, the input parameters to the codes (e.g. device geometry and wave parameters), the requested outputs (e.g. device motions), and preliminary simulation results are presented. Finally, important conclusions are made, lessons learned are noted, and future work is identified.

III. PARTICIPANTS AND CODES

The participants in the WEC3 project are InWave, WaveDyn, ProteusDS, and WEC-Sim. An overview of the features of the participating codes presented in Table 1, and visualizations of simulations from the different codes are shown in Figure 1.

Table 1. WEC3 Code Feature Comparison (under development).*

| Code Name | InWave | WaveDyn | ProteusDS | WEC-Sim v1.0 |
|---|---|--|--|---|
| Code Developer | INNOSEA/ECN | DNV GL | DSA | NREL/SNL |
| Multibody Mechanics | Relative coordinate algorithm | Proprietary multibody method | Articulated Body Algorithm | SimMechanics |
| Hydrodynamics | Linear potential, Nonlinear Froude-Krylov | Linear potential, Nonlinear Froude-Krylov* | Linear potential, Nonlinear Froude-Krylov | Linear potential, Nonlinear Froude-Krylov* |
| BEM Solver | Integrated (NEMOH) | Multiple options (inc. WAMIT and AQWA) | Multiple options (inc. WAMIT and SHIPMO3D) | Multiple options (inc. WAMIT, AQWA, and NEMOH) |
| Hydro-Mechanics Coupling | Relative coordinates | Generalized coordinates | Generalized coordinates | Generalized coordinates |
| Hydrostatics | Linear*, Nonlinear | Linear, Nonlinear | Linear, Nonlinear | Linear, Nonlinear* |
| Body-to-Body Hydrodynamic Interactions | Yes | Yes | Yes* | Yes* |
| Viscous Drag Formulation | Morison elements with relative velocity | Morison elements with relative velocity | Morison elements with relative velocity | Quadratic damping using body velocity, Morison elements with relative velocity* |
| Mooring (Linear Stiffness/Quasi-Static/Dynamic) | Yes/Yes/No | Yes/Yes/No | Yes/No/Yes | Yes/No/No |
| PTO and Control | Linear, Look-up table, and API | Linear and API | Linear, PID control, and API | User-defined in MATLAB/Simulink |
| License | Commercial | Commercial | Commercial | Apache 2.0 |
| External Software | None | None | None | MATLAB, Simulink, SimMechanics |

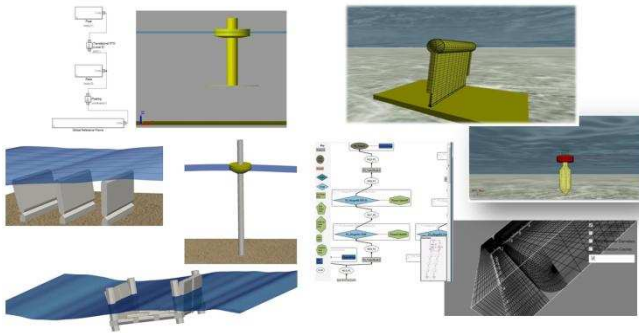


Figure 1. Visualization of some of the numerical models

A. InWave

InWave is a multi-body offshore numerical tool with a WEC design dedicated interface. This software is developed by INNOSEA and Ecole Centrale de Nantes.

InWave is based on the tight coupling of a multibody mechanical solver and a hydrodynamic potential flow solver.

The fully non-linear mechanical solver uses relative coordinates. It walks recursively along the multibody tree structure to build and solve the equations of motion. The description of the multibody structure uses the modified Denavit-Hartenberg parameterisation [3].

The mechanical solver is tightly coupled with a linear potential flow solver [4] also using articulation coordinates. Doing so, the number of elementary diffraction/radiation problems to solve is reduced [5] and hydrodynamic interactions are accounted for.

In addition, *InWave* is self-contained: there is no need for an external program to use *InWave*. All the relevant solvers (including BEM, PTO and Moorings) are integrated in a series of modules that the user runs step by step.

Code to code verification [6] and validation against experiments [7] has been carried out for InWave, achieving the proof-of-concept phase.

B. WaveDyn

WaveDyn is a multi-body, time-domain, simulation tool developed by DNV-GL specifically for evaluating WEC performance.

The software allows a user to construct a numerical representation of a WEC by connecting structural, hydrodynamic, power take-off (PTO) and mooring components using a flexible user interface. Single machines may be modeled in isolation, or a user may choose to build a multiple WEC simulation model for a known array layout. Control actions may be implemented through the PTO components, and simulations may be run with regular or irregular input sea states, for multiple wave directions.

The hydrodynamics module in its most basic form is a quasi-linear formulation based on a boundary element method (BEM), potential flow solver such as WAMIT. Diffraction, radiation, hydrostatic and viscous effects are included in the model. Additional nonlinear forcing terms may be included

for the excitation and hydrostatic forces but these are subject to ongoing validation. The completion of calculations in the time-domain, allows nonlinear forces and structural elements to be modeled. Results obtained for models exhibiting a linear response (or those that are close enough to be assumed linear) can be processed to build up frequency response data, such as response amplitude operators (RAOs) or relative capture widths (RCWs).

WaveDyn has already been subject to a number of validation campaigns against experimental measurements on various device types, scales, in isolation or in array [8]–[10].

C. ProteusDS

ProteusDS is a dynamic analysis software package that is used for marine, offshore, and subsea applications. It features a graphical user interface and 3D visualizations of simulations. Being a general multi-body dynamics solver, it is employed by offshore oil and gas [11], aquaculture [12], marine renewable [13], naval architecture, oceanography, and other offshore engineering industries to solve a variety of problems. It allows the testing of virtual prototypes of systems that are exposed to extreme wind, current and waves – which reduces risk and enables system optimization.

It uses the articulated body algorithm (ABA) to solve the forward dynamics problem for articulated rigid bodies in a generalised way. A significant advantage of this method is its efficiency; the computational complexity grows linearly with the number of sequential links [14]. The ABA effectively reduces the degrees of freedom of downstream link rigid bodies to the number of degrees of freedom of their upstream joint.

Forward speed dependent boundary element method (BEM) solutions are supported which enables the modelling of manoeuvring ships, and bodies exposed to tidal currents.

ProteusDS also provides a control system modelling infrastructure. This is supplemented by an application programmer interface (API), which allows users the flexibility of generating their own models and custom control systems.

Most notably, ProteusDS features cubic-spline based finite element cable and net models for modelling non-linear moorings, power cables, pipelines, and fish farm systems.

D. WEC-Sim

WEC-Sim (Wave Energy Converter Simulator) is an open source wave energy converter simulation tool jointly developed by Sandia National Laboratories and the National Renewable Energy Laboratory with support from the US Department of Energy. The WEC-Sim code is developed in MATLAB/SIMULINK using the multi-body dynamics solver SimMechanics. WEC-Sim has the ability to model devices that are comprised of rigid bodies, joints, motion constraints, with power-take-off and mooring systems. Simulations are performed in the time-domain by solving the governing WEC equations of motion in 6 degrees-of-freedom using the Cummins' formulation [15].

WEC-Sim v1.1 is freely available through the WEC-Sim GitHub website [16]. WEC-Sim has undergone extensive verification through code-to-code comparison and preliminary

experimental validation [17], [18]. Further experimental validation of the WEC-Sim code is planned for fall 2015.

IV. METHODOLOGY

Phase I of the WEC3 project consists of the numerical code-to-code comparison described in this section.

A. Device Selection

A Floating three-body Oscillating Flap device (F3OF) was chosen as the reference test case for several reasons. This device, inspired by the Langlee system, was defined and studied in detail in [19]. It is particularly well suited to benchmark the WEC dedicated codes as it features the following:

- Fully floating device
- Presence of a mooring system
- Unusual degrees of freedom (flap rotations)
- Important body-to-body hydrodynamic interactions between flaps
- Viscous drag is an important source of damping

Therefore, this test case is challenging to numerically model. Moreover, modelling the Langlee device tests the codes abilities to model numerous physical phenomena that are of direct relevance to WEC modelling. In the following section, detailed specification of this system and the load cases considered in the code-to-code comparison are provided.

B. System Specifications

The F3OF device is made of a semi-submersible base supporting 2 flaps. The base is moored and the mooring system is modelled with an equivalent linear stiffness in surge only. The surge stiffness and other relevant device specifications are defined in Table 2,

Each flap consists of 2 rigidly linked rectangular plates. The flaps can only move relative to the base about their revolute joint (see Figure 2). A power take-off (PTO) is acting on each joint. The equivalent linear damping of the PTO is defined in Table 2.

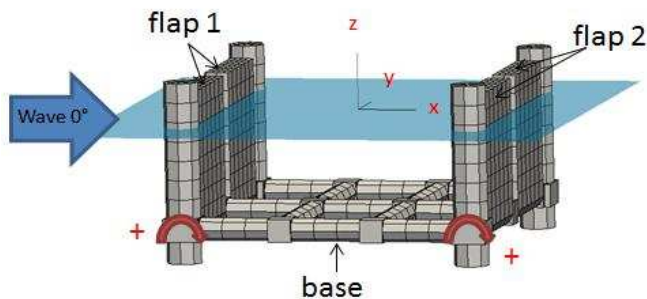


Figure 2. Schematic of the F3OF inspired by the Langlee device

Table 2. Dimensions and mechanical parameters of the F3OF.

| | Base | Flap 1 | Flap 2 |
|---|----------|----------|----------|
| Length along X (m) | 27 | 2 | 2 |
| Length along Y (m) | 27 | 9.5+9.5 | 9.5+9.5 |
| Length along Z (m) | 16 | 13 | 13 |
| Draft (m) | 12 | 10 | 10 |
| hinge - X position (m) | x | -12,5 | 12,5 |
| hinge - Y position (m) | x | 0 | 0 |
| hinge - Z position (m) | x | -9 | -9 |
| mass (kg) | 1089825 | 179250 | 179250 |
| COG - X position (m) | 0 | -12,5 | 12,5 |
| COG - Y position (m) | 0 | 0 | 0 |
| COG - Z position (m) | -9 | -5,5 | -5,5 |
| pitch inertia around each body COG (kg.m ²) | 7,63E+07 | 1,30E+06 | 1,30E+06 |
| Mooring stiffness (N/m) | 1,00E+05 | x | x |
| PTO damping (N.m.s) | x | 4,00E+07 | 4,00E+07 |
| Water depth (m) | infinite | | |

For all simulations, the water depth is assumed infinite and the water density is set to 1025 kg/m³. All waves were set to propagate with a heading of 0° along x-axis, as shown in Figure 2.

C. Load Cases Specifications

The load cases and system configurations used for comparison of simulation results are defined in Table 3. First, the hydrodynamic coefficient databases (HDB) were independently determined by the participants using their chosen BEM solver. Coefficients from each of the participants are compared in Section V. Each participant then performed decay tests to validate their results against each the others. These tests verify that the models are in agreement with regards to the model inertia, hydrostatic model, mooring model and wave radiation loading. It also highlights the differences between viscous drag models used by each code.

Currently, the WEC3 participants are developing response amplitude operators (RAOs) for the F3OF device by performing regular wave simulations at various frequencies. By generating RAOs at two different wave amplitudes, nonlinear effects on device performance will be studied. Simulations in irregular waves will then be performed to allow comparison in terms of response spectrum. Details of the wave conditions considered are provided in Table 4.

Table 3-Specifications of load cases.

| Type of test | Description | Case | Initial position | Configuration |
|-------------------|----------------------|----------------------|--------------------------|---|
| Hydrostatic test | Hydrostatic test | HS1 | as given in input meshes | x |
| | Surge | DT1 | SURGE = +5m | Flaps locked No viscous drag |
| | | Pitch | DT2 | PITCH = +10 deg |
| Decay tests | Flap1 | DT3 | FLAP1 = +10 deg | Base locked No viscous drag PTO OFF |
| | Surge - viscous drag | DT4 | SURGE = +5m | Flaps locked viscous drag |
| | | Pitch - viscous drag | DT5 | PITCH = +10 deg |
| | Flap1 - viscous drag | DT6 | FLAP1 = +10 deg | Base locked |
| | | | | viscous drag PTO OFF |
| | Regular waves | Small waves for RAO | REG1-REG20 | Equilibrium position |
| Big waves for RAO | | REG21-REG40 | Equilibrium position | viscous drag |
| Irregular waves | Small sea state | IRREG1 | Equilibrium position | viscous drag |
| | Bigsea state | IRREG2 | Equilibrium position | viscous drag |

Table 4-Wave conditions for the load cases.

| Type of test | Description | Case | A or Hs | T or Tp | γ | β |
|-----------------|---------------------|-------------|----------|--------------------|----------|---------|
| | | | [m] | [s] | | [°] |
| Regular waves | Small waves for RAO | REG1-REG20 | A = 0.01 | T = 1 - 20 each 1s | - | 0 |
| | Big waves for RAO | REG21-REG40 | A = 1 | T = 1 - 20 each 1s | - | 0 |
| Irregular waves | Small sea state | IRREG1 | Hs = 1 | Tp = 10 | 3,3 | 0 |
| | Big sea state | IRREG2 | Hs = 3 | Tp = 12 | 3,3 | 0 |

V. PRELIMINARY RESULTS

A. Hydrodynamic Database

This section provides a comparison of the hydrodynamic coefficients produced by the five participants. Only the added mass coefficients are provided here for brevity, although the wave radiation damping coefficients have also been compared and show similar trends.

The datasets of the five participants are labelled:

- “INW” (InWave),
- “PDS” (ProteusDS),

- “WDN” (WaveDyn), and
- “WSM” (WecSim).

Each participant generated a database of hydrodynamic coefficients using their potential flow solver of choice. The INW participant generated their coefficients using InWave, which fully integrates NEMOH, while the remaining participants generated their coefficients using WAMIT. The group of participants that used WAMIT independently ran simulations to determine the required hydrodynamic coefficients. Identical mesh files were used for the WAMIT and NEMOH simulations. Results from each participant are presented in Figure 3 – Figure 6.

The INW participant modelled the multi-body system using a relative coordinate system giving their system a total of 8 degrees of freedom (DOF). Their hydrodynamic coefficients are produced as matrices of size 8x8. Some of the other participants are also employing 8 DOF relative coordinate multi-body system models, however they are all expressing their hydrodynamic coefficients based on three individual 6DOF rigid bodies producing a total of 18 independent DOFs and thus size 18x18 matrices of wave radiation coefficients.

For the purpose of comparison, both the WAMIT and NEMOH produced hydrodynamic databases (18 DOF solutions) were reduced to produce a database equivalent to INW’s (8 DOF solution) and are described with respect to INW’s reference frames.

As shown in Figure 3 – Figure 6, the INW, WSM, and PDS match very well, thus verifying the performance of both WAMIT and NEMOH and providing confidence in the HDB results. There are minor differences in the coefficients, however, these aren’t expected to produce any significant differences in time domain simulation results. The WDN results differed more significantly from the other participants, suggesting that the solver settings used by the WDN group were slightly different from the other participants. At the time of press, the WEC3 team is still investigating the cause of this discrepancy, however, it is expected that once solver settings for the WDN WAMIT runs are adjusted the WDN hydrodynamic coefficients will fall in line with those of the other participants.

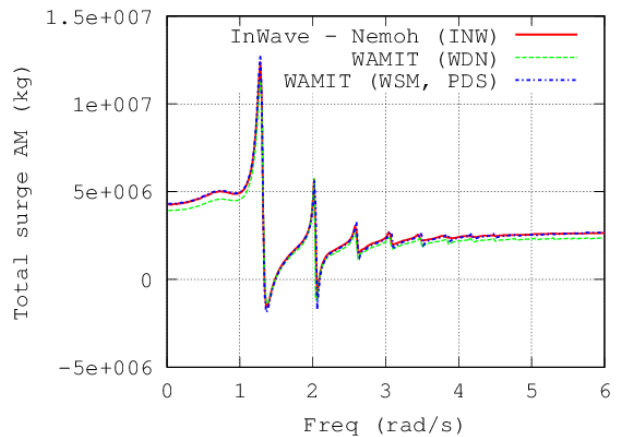


Figure 3. Total surge added mass.

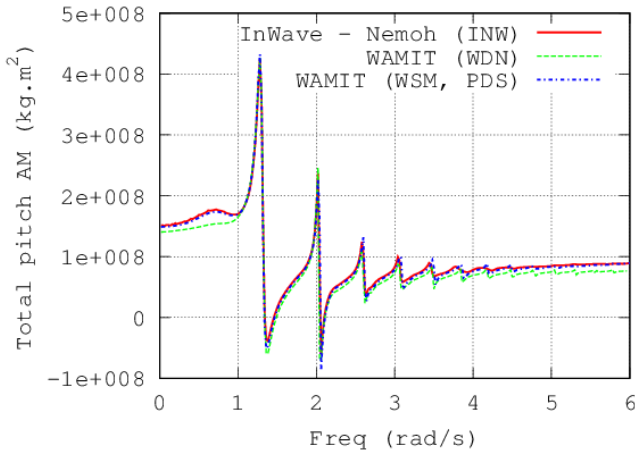


Figure 4. Total pitch added mass.

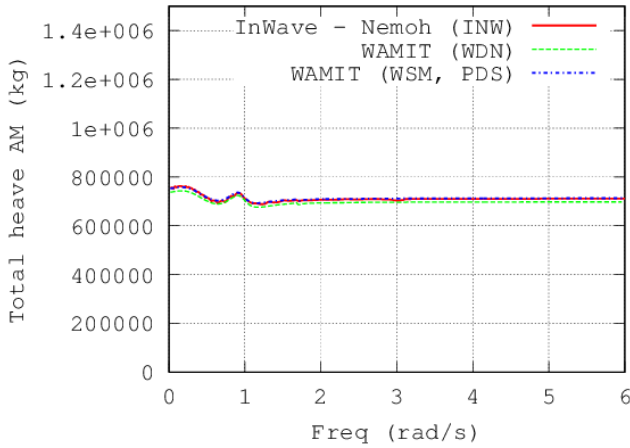


Figure 5 Total heave added mass.

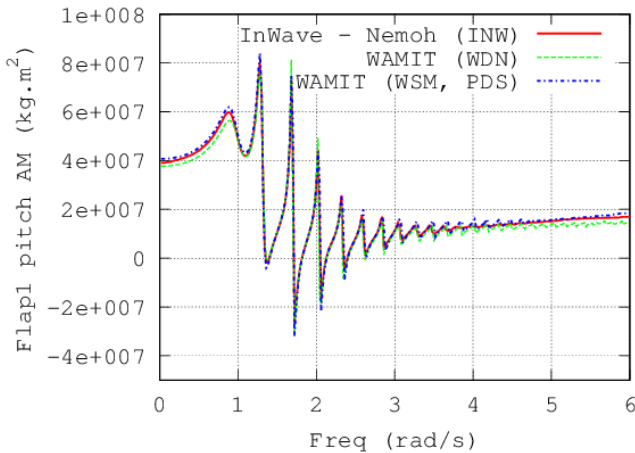


Figure 6. Flap 1 pitch added mass.

The INW reference frame used for the base body and the combined coefficients is located at the CG of the base with a frame orientation equal to the inertial frame. The reference frames for the two flaps are located at their respective joints and at the centre of the body along the Y-axis. Their frames also have the same orientation as the inertial reference frame.

Figure 3 - Figure 5 show a comparison of the total frequency dependent added mass coefficients due to wave radiation, expressed about the INW reference frame. Figure 3 shows the total surge added mass, which for the 18 DOF set of coefficients, is the sum of the surge-surge coefficients for the base, flap 1 and flap 2 bodies as well as the sum of the respective surge-surge coefficients due to multi-body interaction. For these total coefficients, it's assumed that the joints are locked and the 3 bodies are moving as a single rigid body. Figure 4 and Figure 5 are the total coefficients for the pitch-pitch and heave-heave degrees of freedom respectively. Finally, Figure 6 shows the pitch-pitch added mass coefficients for flap 1 only, pitching about its joint; the other bodies are not radiating waves and thus are not contributing to these coefficients.

| ω (rad/s) | λ (m) | L/λ |
|------------------|---------------|-------------|
| 1.29 | 36.47 | 2/3 |
| 1.66 | 22.37 | 1 |
| 2.02 | 15.11 | 1.5 |
| 2.32 | 11.45 | 2 |
| 2.59 | 9.19 | 2.5 |
| 2.85 | 7.59 | 3 |
| 3.06 | 6.58 | 3.5 |
| 3.30 | 5.66 | 4 |
| 3.49 | 5.03 | 4.5 |

Table 5. Frequency of peaks in flap1 pitch radiation coefficients, their corresponding wave lengths and the number of wavelengths that fit between the flaps. L is the distance between the inside faces of the two flaps; effectively 23m.

The peaks seen in surge and pitch, and the distance between them in terms of frequency, are dependent on the wavelength and the distance between the two flaps. Table 5 contains the frequencies of the peaks, the corresponding wavelength at that frequency assuming the deep water dispersion relation, as well as the number of wavelengths that fit between the paddles. These peaks occur because the wave flap 1 is radiating is reflecting off flap 2 and super positioning over itself on the way back causing constructive interference at particular frequencies, and destructive interference at other frequencies. Figure 7 and Figure 8 illustrate this for frequencies of 1.66 rad/s and 2.02 rad/s.

There are twice as many peaks present in Figure 6 than in Figure 3 and Figure 4 where all three bodies are assumed to be moving together as a single rigid body in a locked fashion. This is because destructive interference occurs when accounting for the effect the radiated waves of flap 2 on flap 1 and vice versa as seen in Figure 7 and Figure 8.

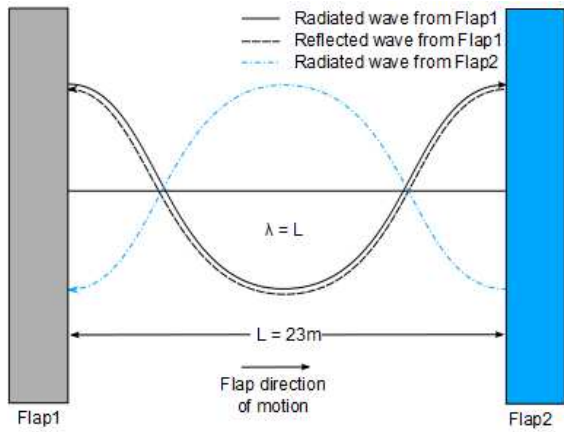


Figure 7. Wave radiation at a frequency of 1.66 rad/s resulting in wavelengths of $\lambda = L$.

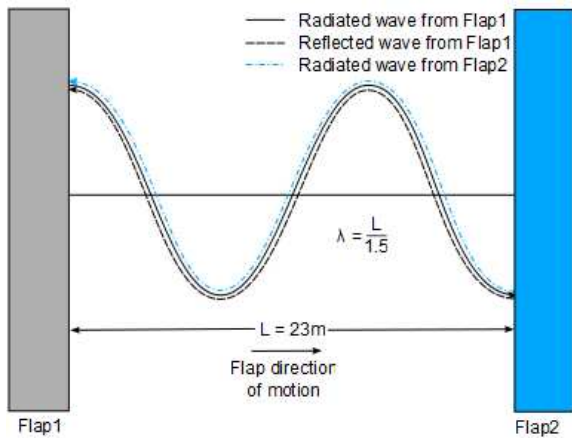


Figure 8. Wave radiation at a frequency of 2.02 rad/s resulting in wavelengths of $\lambda = L/1.5$.

B. Decay Tests

Decay tests have been performed with and without viscous drag to clearly identify differences coming from viscous drag models. The decay tests conducted here are outlined in Table 3.

1) Without viscous drag

The first decay test is a surge decay test. The flaps are considered locked to the base. The response in surge is compared. The decay frequency is determined mainly by the added mass the at surge natural frequency and the surge mooring stiffness, as the radiation damping at the surge frequency is relatively small compared to critical damping. Figure 9 shows a fair match between participants for the first few oscillations, however after several oscillations the PDS and WSM results diverge from the INW and WDN results. The WSM results show a different natural period, suggesting that the mass, added mass, or mooring spring stiffness is modelled differently from the INW and WDN simulations, while the PDS frequency and decay rate is different from the results of the other groups. The exact cause of this

discrepancy has not yet been determined and further investigation of this behaviour is left for future work.

A pitch decay test was next performed, keeping the flaps locked. The response to this test is driven by pitch added mass, radiation damping at the pitch natural frequency, and the pitch hydrostatic stiffness. Figure 10 shows that all models are in good agreement and that there is significant radiation damping that quickly reduces the magnitude of oscillation with time.

The last decay test is a flap decay test with a fixed base. The flap 1 initial position is set to 10° . Both Flap 1 and Flap 2 response are compared. Figure 11 shows a good agreement for Flap 1 response for INW/PDS/WDN. INW shows a slight difference in term of flap natural period. This might be due to small differences in HDB due to the different potential flow solver used. It can be observed that after a few periods, WSM differs significantly from the other solvers prediction. The motion response steadily increases with time whereas the other software predicts decreasing amplitude for roughly the first 200s and then increasing amplitude until the end of the simulation. The difference between WSM and the other codes is being investigated.

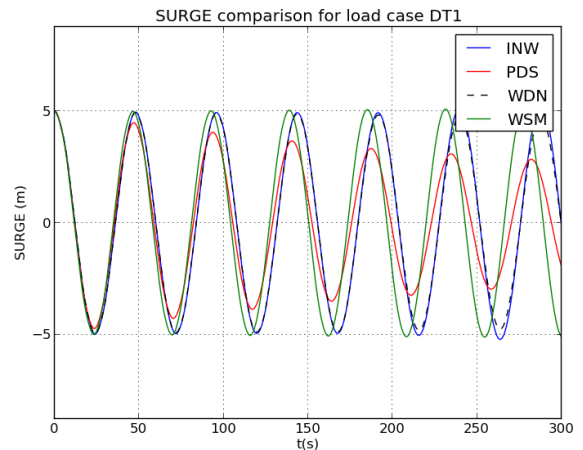


Figure 9. Comparison of surge motion for load cast DT1.

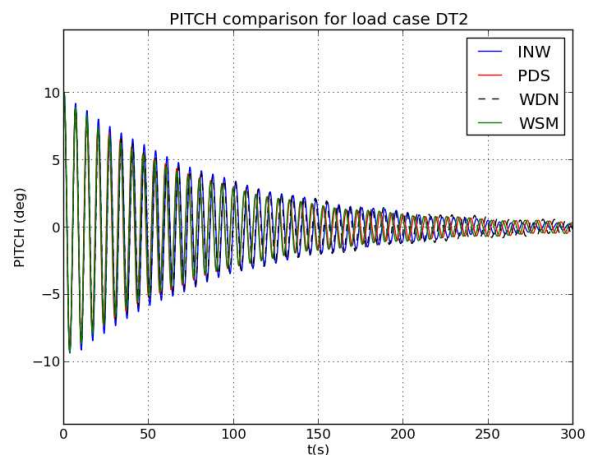


Figure 10. Comparison of pitch motion for load case DT2.

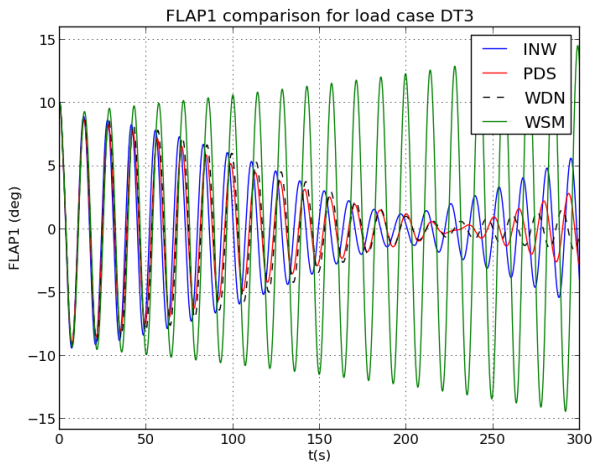


Figure 11. Comparison of Flap 1 pitch motion for load case DT3.

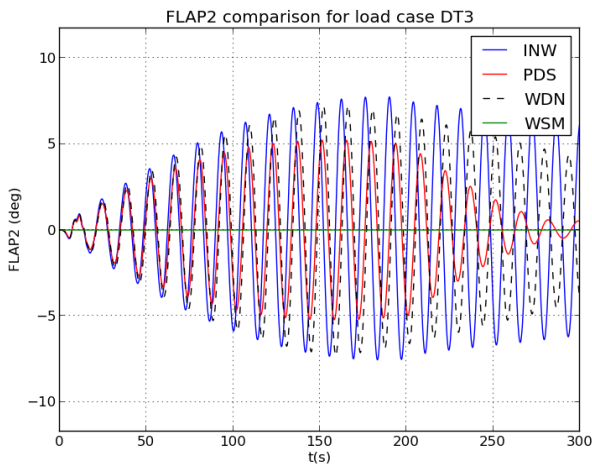


Figure 12. Comparison of Flap 2 pitch motion for load case DT3.

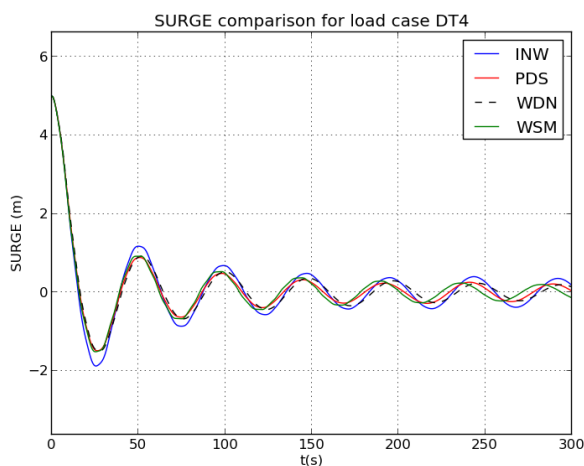


Figure 13. Comparison of surge motion for load case DT4.

It is interesting to note that flap 1 oscillations are damped until around 200s before increasing again. This is clearly due to hydrodynamic interactions between the two flaps as highlighted in part IV.5.

When flap 1 is moving, it creates a wave that is exciting flap 2. This wave reflects on flap 2 and come back to flap 1. In addition, flap 2 is starting to move (see Fig 12) which in turn will excite flap 1.

Figure 12 shows the same behaviour for INW/PDS/WDN. INW/WDN show a fair agreement in term of amplitude of response for flap 2. INW flap 2 natural period is slightly different from PDS/WDN as it was for flap 1. WSM does not implement hydrodynamic interactions between bodies in the version of the code used in this project, therefore, flap 2 response is zero in this case.

2) With viscous drag

The same decay tests were run with corrections for the modelling of viscous drag. The corrections differ in each model. All models are using a drag coefficient of 1.0 for the base body and of 8.0 for the flaps.

The INW drag model is based on Morison formulation using relative velocity between the bodies and the fluid. The pipes constituting the base are modelled as series of cylinders with 1m length elements. The same formulation is used on the flaps that are discretised vertically with 1m height elements.

The PDS drag model is based on Morison formulation using relative velocity between the bodies and the fluid. It uses a mesh-based approach for determining the drag loads.

The WDN drag model is based on Morison formulation using relative velocity between the bodies and the fluid. The pipes constituting the base and the flaps are modelled as series of cylinders.

The WSM simulations used a quadratic loading model using based the body's velocity sampled at the CG where the load is also applied at the CG.

Figure 13 shows good agreement between the codes for this surge decay test. This was expected as in case of surge motion only, as the body velocity is the same at every point of the structure. That is, the location of the centre of distribution of the viscous drag load plays a minor role when motion is mainly in surge.

Figure 14 shows how differences appear for pitch. The body velocity is not the same everywhere on the structure. Drag models are quadratically dependent on velocity, thus models that integrate the drag load over a body using Morison elements will produce a different load than quadratic loading based models that compute the drag load using a velocity sampled at a single point. Similarly, the location of the centre of pressure of these loads has an effect on the resulting moment acting about the flap's joint. Different drag models lead to different damping rates and thus different amplitude of motion. The least damping is obtained with WSM, then with WDN. PDS and INW results are very close which was expected as they are using a similar approach to modelling the viscous drag.

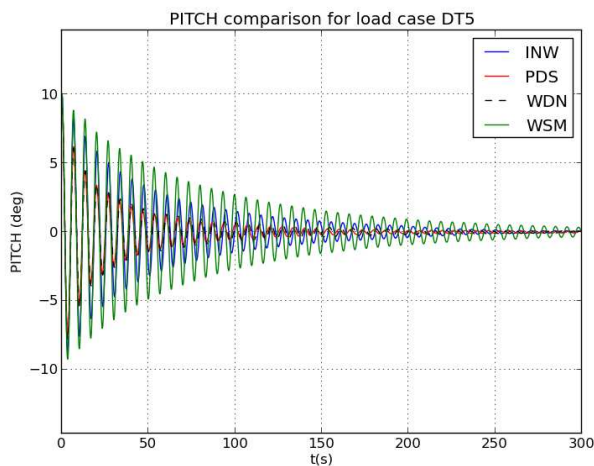


Figure 14. Comparison of pitch motion for load case DT5.

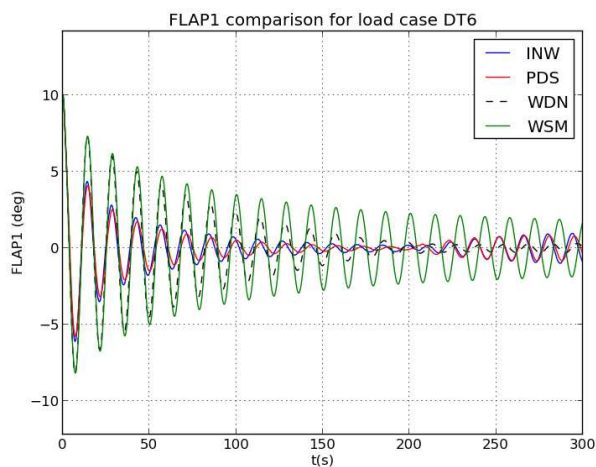


Figure 15. Comparison of Flap 1 pitch motion for load case DT6.

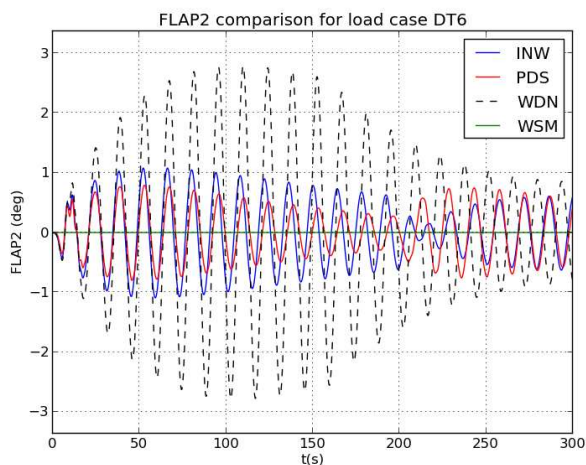


Figure 16. Comparison of Flap 2 pitch motion for load case DT6.

Figure 15 and Figure 16 a good agreement for the Flap 1 pitch motion between INW/PDS results on one hand, and between WSM/WDN results on the other. This was expected as the modelling approach for viscous drag corrections are different between the two groups of codes. For Flap 2, Figure 16 the agreement between WSM/WDN is quite fair. Overall, the motion response is considerably reduced in comparison with the case without viscous correction.

VI. CONCLUSION AND FUTURE WORK

Our work to date on WEC3 allows us to make some observations and preliminary conclusions about the code-to-code comparison phase of the project:

- Overall there is good agreement in the numerical predictions from the 4 participants. The participants that used the same HDB obtained very similar results (see Figure 9 and Figure 10) even though they were using different mechanical solvers.
- Without viscous corrections, largest differences were observed between codes that take into account hydrodynamic body-to-body interactions and those that don't (Figure 10). It highlights that for articulated multibody WECs, it is important to take into account the hydrodynamic interactions.
- Participants have different approach for taking into viscous effects through corrective terms. It is observed that it leads to difference in numerical predictions that can be significant (Figure 13 and Figure 14).

In future work on Phase I, regular and irregular waves will be simulated. In addition, the WEC3 team will explore the sensitivity of power absorption calculations to the difference numerical modelling methods. Information gained from this power absorption comparison will provide valuable insight on the reliability of using numerical modelling tools to estimate power capture from WEC devices. Moreover, these comparisons will help identify if further research and development is needed to improve existing WEC numerical models so that they can reliably be used to assess WEC power performance characteristics.

Phase II of this project will include validation against experimental data sets. Some available experimental databases have been identified. They are experimental results for 1/12 scale model tests of the SEAREV wave energy converter that were conducted in Ecole Centrale de Nantes in France and model tests of a two-body heaving wave energy converter that were conducted at the University of Victoria in Canada.

REFERENCES

- [1] K. Gunn and C. Stock-Williams, "Quantifying the global wave power resource," *Renew. Energy*, vol. 44, pp. 296–304, 2012.
- [2] W. Popko, F. Vorpahl, A. Zuga, M. Kohlmeier, J. Jonkman, A. Robertson, T. J. Larsen, A. Yde, K. S\aa etertr\o, K. M. Okstad, and others, "Offshore Code Comparison Collaboration Continuation (OC4), Phase 1-Results of Coupled Simulations of an Offshore Wind Turbine With Jacket Support Structure," in *The Twenty-second International Offshore and Polar Engineering Conference*, 2012.

- [3] F. Rongère and A. H. Clément, “Systematic dynamic modeling and simulation of multibody offshore structures: Application to wave energy converters,” in *ASME 2013 32nd International Conference on Ocean, Offshore and Arctic Engineering*, 2013, pp. V005T06A086–V005T06A086.
- [4] A. Babarit and G. Delhommeau, “Theoretical and numerical aspects of the open source BEM solver NEMOH,” in *Proc. Of the 11th European Wave and Tidal Energy Conference*, Nantes, France, 2015.
- [5] A. Combourieu, M. Philippe, F. Rongère, and A. Babarit, “InWave: A New Flexible Design Tool Dedicated to Wave Energy Converters,” in *ASME 2014 33rd International Conference on Ocean, Offshore and Arctic Engineering*, 2014, pp. V09BT09A050–V09BT09A050.
- [6] V. Leroy, A. Combourieu, M. Philippe, F. Rongère, and A. Babarit, “Benchmarking of the New Design Tool InWave on a Selection of Wave Energy Converters from NumWEC Project,” in *Asian Wave and Tidal Energy Conference*, Tokyo, Japan, 2014.
- [7] A. Combourieu, M. Philippe, A. Larivain, and J. Espedal, “Experimental Validation of InWave, a Numerical Design Tool for WECs,” in *11th European Wave and Tidal Energy Conference*, Nantes, France, 2015.
- [8] E. B. L. Mackay, J. Cruz, M. Livingstone, and P. Arnold, “Validation of a Time-Domain Modelling Tool for Wave Energy Converter Arrays,” in *European Wave and Tidal Energy Conference*, Aalborg, Denmark, 2013.
- [9] E. Mackay, J. Cruz, C. Retzler, P. Arnold, E. Bannon, and R. Pascal, “Validation of a new wave energy converter design tool with large scale single machine experiments,” in *1st Asian Wave and Tidal Conference Series*, 2012.
- [10] J. Lucas, M. Livingstone, M. Vuorinen, and J. Cruz, “Development of a wave energy converter (WEC) design tool—application to the WaveRoller WEC including validation of numerical estimates,” in *4th International Conference on Ocean Energy*, 2012, vol. 17.
- [11] D. M. Steinke, R. S. Nicoll, and A. R. Roy, “Real-Time Finite Element Analysis of a Remotely Operated Pipeline Repair System,” in *ASME 2013 32nd International Conference on Ocean, Offshore and Arctic Engineering*, 2013, pp. V04AT04A006–V04AT04A006.
- [12] R. S. Nicoll, D. M. Steinke, J. Attia, A. Roy, and B. J. Buckham, “Simulation of a high-energy finfish aquaculture site using a finite element net model,” in *ASME 2011 30th International Conference on Ocean, Offshore and Arctic Engineering*, 2011, pp. 35–44.
- [13] R. S. Nicoll, C. F. Wood, and A. R. Roy, “Comparison of physical model tests with a time domain simulation model of a wave energy converter,” in *ASME 2012 31st International Conference on Ocean, Offshore and Arctic Engineering*, 2012, pp. 507–516.
- [14] R. Featherstone, *Rigid body dynamics algorithms*. Springer, 2014.
- [15] Cummins, WE, “The Impulse Response Function and Ship Motions,” David Taylor Model Basin-DTNSRDC, 1962.
- [16] Michel Lawson, Kelley Ruehl, Yi-Hsiang Yu, Carlos Michelen, and Nathan Tom, “WEC-Sim,” 2015. [Online]. Available: <http://wec-sim.github.io/WEC-Sim/>.
- [17] K. Ruehl, C. Michelen, S. Kanner, M. Lawson, and Y.-H. Yu, “Preliminary Verification and Validation of WEC-Sim, an Open-Source Wave Energy Converter Design Tool,” in *33rd International Conference on Ocean, Offshore and Arctic Engineering, OMAE, San Francisco, CA, United States (Abstract accepted)*, 2014.
- [18] Y.-H. Yu, Y. Li, K. Hallett, and C. Hotimsky, “Design and analysis for a floating oscillating surge wave energy converter,” in *ASME 2014 33rd International Conference on Ocean, Offshore and Arctic Engineering*, 2014, pp. V09BT09A048–V09BT09A048.
- [19] A. Babarit, J. Hals, M. J. Muliawan, A. Kurniawan, T. Moan, and J. Krokstad, “Numerical benchmarking study of a selection of wave energy converters,” *Renew. Energy*, vol. 41, pp. 44–63, 2012.